Artigo Original

Revista Brasileira de Física Médica (2022) 16:685

Estimativa de dose em CT utilizando *phantom* ICRU/AAPM

CT dose estimations using the ICRU/AAPM phantom

Yuri N. de Stefani, Denise Y. Nersissian, Paulo R. Costa[1]

[1]Instituto de Física, Universidade de São Paulo, 05508-090, São Paulo, Brasil

Resumo

Um método proposto para obter a dose em Tomografia Computadorizada foi avaliado em um *phantom* longo, feito de polietileno. Este *phantom* tem um comprimento de 600 mm. Adotando uma função empiricamente caracterizada $h(L)$, a tendência do crescimento assintótico da dose pelo aumento da varredura pode estimar uma dose em uma varredura de tamanho infinito para uma única rotação axial do tubo de raios X. A curva de $h(L)$ foi estimada para diferentes protocolos clínicos: tensão, pitch, *Head/Body* e medições de centro/periférico. O *phantom* de ultra alta massa molecular de 600 mm de comprimento, chamado de *phantom* ICRU/AAPM, foi proposto por uma parceria entre ICRU e AAPM (*Task Group* 200). Este comprimento permite realizar uma varredura maior do que *phantom* de PMMA para $CTDI_{100}$, cuja medição é de 100 mm. A medida do *phantom* ICRU/AAPM foi realizada em tomógrafos da General Electric, Toshiba e Philips. As medições foram feitas com uma câmara de ionização pequena inserida no centro ou periferia do *phantom* e as métricas da função $h(L)$ (dose de equilíbrio, comprimento de equilíbrio, fração de espalhamento) foram obtidas. Uma única medição demonstrou ser suficiente para obter a função $h(L)$.

Palavras-chave: tomografia computadorizada, dosimetria, dose de equilíbrio, *phantom*.

Abstract

A proposed method to obtain the dose for Computed Tomography was evaluated on long a phantom, made of polyethylene. This phantom is 600 mm large. Adopting an empirical characterized function $h(L)$, a tendency of the asymptotical grow of the dose by the increase of the scanning length can estimate the dose in an infinite scanning length for a single axial rotation of the x-ray tube. The curve of $h(L)$ was estimated for different clinical protocols: tension, pitch, head/body, and center/peripheral measurements. The ultrahigh molecular weight polyethylene phantom of 600 mm length, named ICRU/AAPM phantom, was proposed by a partnership between ICRU and AAPM (Task Group 200). This length provides a higher scanner length then PMMA phantom for $CTDI_{100}$, whose measurement is 100 mm. The measures of ICRU/AAPM phantom were performed on General Electric, Toshiba, and Philips scanners. The measurement was performed on a thimble ion chamber inserted in the center or periphery of the phantom. Using the measurements, $h(L)$ functions (equilibrium dose, equilibrium length and scatter fraction) were obtained. A single scan has been demonstrated to be sufficient to obtain the $h(L)$ function.

Keywords*: computed tomography; dosimetry; equilibrium dose, phantom.*

1. Introduction

The computed tomography is one of the most important technique for diagnostic imaging. Due to its use of ionizing radiation, it is necessary estimate the dose of clinical protocols. A practical indicator is the Computed Tomography Dose Index (CTDI), which has been used for decades. It is defined as the dose measured on a single axial rotation. CTDI_{100} is the measured on 100 mm length using a pencil chamber. It was generalized as “weighted average”, $CTDI_w$, which is a mean value between the measurement on the center and on the peripheral (1). After the adoption of multi-slice detector CT (MDCT), a new CT dose quantity was introduced (2), the volumetric-CTDI, $\mathrm{CTDI}_{\mathrm{vol}}$, which is the division of $\mathrm{CTDI}_{\mathrm{w}}$ and the corresponding pitch. This dose quantity represents the estimative of the average dose on a unit of volume. All those units are derived from CTDI_{100}.

Compared to an ideal infinite large chamber, Boone defined an efficiency ε for the CTDI_{100}. According to Boone, for 10 mm slice thickness, voltage of 120 kV, the efficiency, for Head phantom of CTDI_{100}, are 66% and 88% for central and peripheral, respectively. Due to the evolution of CT through the last decades, the use of CTDI_{100} for dosimetry becomes unsuitable (3).

A new paradigm for dosimetry theory was described on AAPM report 111 (4), which proposes a measurement on a large phantom to estimate the dose on an ideal infinite large phantom (*equilibrium dose*). The methodology implies the measurement on the central of the phantom with a thimble ion chamber. The methodology allows to estimate the dose distribution over the scanning length. With this methodology, it is possible to estimate the maximum dose. On ICRU 87 (5), it is shown the design of a new phantom composed of polyethylene, with 600 mm length, for a large measurement. This phantom is adequate for the methodology indicated on AAPM report 111. The technical drawing of this phantom, hereafter referred as ICRU/AAPM phantom, is disclosed on AAPM report 200 (6). Also, on the AAPM report 200, there is also a method to obtain the equilibrium dose. It is also possible to estimate the equilibrium dose using CTDI_{100} phantom. As shown by Costa et al. (7), three CTDI_{100} phantoms were tied together to increase the measure length.

In the present work, the ICRU/AAPM phantom was manufactured, and measurements have been done on scanners of three different vendors. A set of protocols (pitch; voltage; head and body filters; center and peripheral protocols) were evaluated and obtained D_{eq} (equilibrium dose), L_{eq} (*equilibrium length*) and α (*scatter fraction*).

2. Materials and Methods

2.1. ICRU/AAPM Dosimetry Phantom

The new dosimetry phantom proposed by ICRU 87 (with a partnership of AAPM Task Group 200) is long enough to accomplish a measurement on a large scanning length. Its composition is ultra-high molecular weight polyethylene (UHMW), mass density approximately 0.97 g/cm³, with 30 cm of diameter and 60 cm length. It is compound of three sections of 20 cm length each. Each section has a mass around 13.7 kg, resulting on 41.1 kg for the phantom assembled. The AAPM report 200 discloses the technical drawing of the components of the phantom. This phantom was manufactured at the mechanical workshop of the Institute of Physics of the University of São Paulo. The assembled phantom is shown in Figure 1.

Figure 1 - The ICRU/AAPM phantom assembled.

2.2 Thimble ion chamber measurements

The measurement was made using a thimble ion chamber (8) of 0.6 cm³, a 10×6-0.6CT ion chamber (S/N 02– 4831), coupled to a digitizer module, a Accu-Gold+ (model AGDM+, S/N 48–1054). Both the ion chamber and the digitizer module are manufactured by Radcal Corporation.

As described on the AAPM report 111 and 200, the ion chamber is centered on the phantom. Scans of 600 mm were made using different protocols of voltage, pitch, Center/Peripheral and Head/Body in scanners of three vendors: General Electric (GE Discovery CT750HD), Toshiba (Aquilion CXL 128), and Philips (Brilliance 64). The Tables 1-3 show the protocols for General Electric, Toshiba and Philips, respectively. All the measurements were normalized by 100 mAs.

Table 1 - Clinical protocols for GE equipment

	Protocols	
Parameters	Body	Head
Voltage (kV)	80, 100, 120 and 140	80, 100, 120 and 140
Rotation time (s)	1.0	1.0
Pitch	0.516 and 0.984	0.531 and 0.969
Bowtie filter	Body	Head
Collimation (mm)	40	20
Number of selected detectors per rotation	64	32
Detector array width (mm)	0.625	0.625

Font: The authors (2022).

Table 2 - Clinical protocols for Toshiba equipment

	Protocols	
Parameters	Body	Head
Voltage (kV)	80, 100, 120 and 135	80, 100, 120 and 135
Rotation time (s)	1.0	1.0
Pitch	0.641, 0.828 and 1.484	0.656, 0.844 and 1.406
Bowtie filter	Body Standard Axial	Head Brain
Collimation (mm)	32	16
Number of selected detectors per rotation	64	32
Detector array width (mm)	0.5	0.5

Font: The authors (2022).

Table 3 - Clinical protocols for Philips equipment

	Protocols	
Parameters	Body	Head
Voltage (kV)	80, 100, 120 and 140	80, 100, 120 and 140
Rotation time (s)	1.0	1.0
Pitch	0.643, 0.983 and 1.173	0.670 and 0.893
Bowtie filter	Standard B	Standard UB
Collimation (mm)	40	40
Number of selected detectors per rotation	64	64
Detector array width (mm)	0.625	0.625

Font: The authors (2022).

The data was collected through the single method, defined on the AAPM reports 111 and 200, which a single scan can obtain the asymptotical growth of the function scanning length.

It was also collected data through the serial method, defined as well in the AAPM reports 111 and 200, which some scanning lengths are measured on the same protocol. Data using this method was obtained using 120kV, Body protocols, Center and Peripheral protocols, pitch 0.984 for General Electric, 0.828 for Toshiba and 0.983 for Philips. Those data of serial method are used to be compared with the curve obtained using the single method. The data used for analysis are obtained according to the single method.

2.3 Analysis of the measurement

As defined on AAPM reports 111 and 200, the curve experimentally obtained can be fixed by an empirical characterized function. At the function, described by $h(L)$ in Eq. 1:

$$h(L) = D_{eq} \cdot \left(1 - \alpha \cdot e^{-\frac{4 \cdot L}{L_{eq}}}\right). \qquad (1)$$

There are three parameters to be obtained: D_{eq} (*equilibrium dose*), α (*scatter fraction*) and L_{eq} (*equilibrium length*). Those parameters were evaluated using a method described on the Appendix 5 from AAPM report 200. This method adopts an algebraic manipulation the Equation 1 obtaining a linear regression. From the linear and angular coefficients, the parameters L_{eq} and α are acquired.

3. Results

3.1 Validation of the serial and single methods

The Figure 2 shows the comparison between the serial method and the metrics described on Eq.1 for three different companies. It can be seen that the single method can be a good estimation for the serial method. The uncertainty for the serial method, adopting the 10×6-0.6CT ion chamber, is 4% (9).

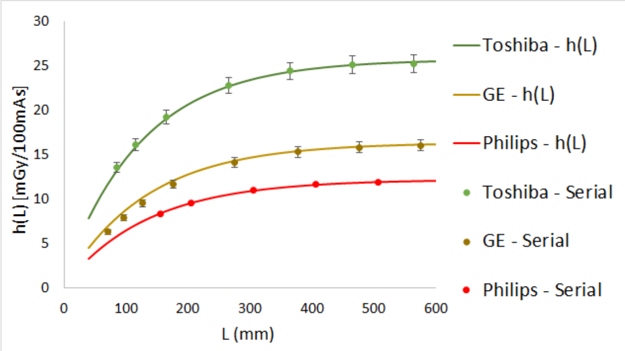

Figure 2 - $h(L)$ function and data from the serial method.

Due to the good results of the implementation of the single method, the data used for analysis are according to the single method, as mentioned in Section 2.2.

3.2 Calculating dose metrics from AAPM report 111 and 200

Figure 3 shows the estimation of measurements for different protocols. All estimations were made using the single method.

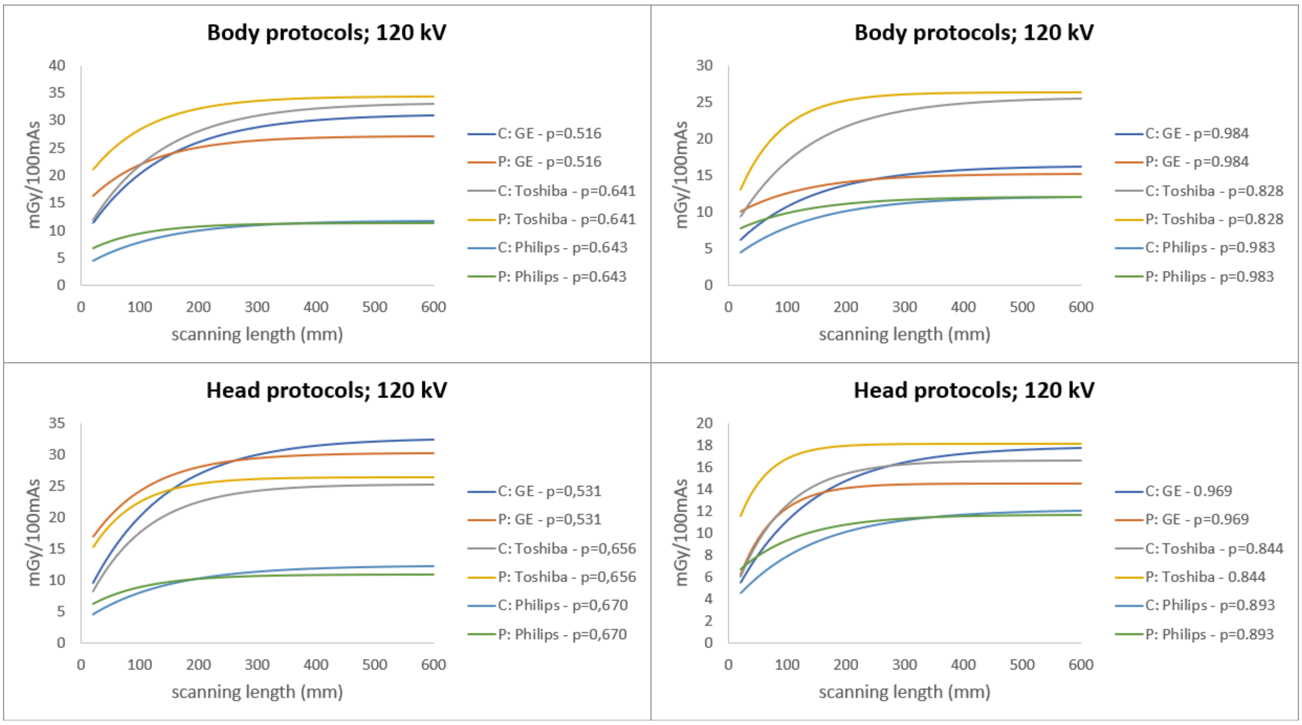

Figure 3 - C: center; P: peripheral. Plot of the h(L) function. All were estimated for 120 kV, Body and Center protocols.

The Tables 4-6 shows the result of the metrics D_{eq}, α and L_{eq} for the General Electric, Toshiba, and Philips scanners. It was calculated the equilibrium dose average D_w, defined as $1/3 \cdot D_{eq,c} + 2/3 \cdot D_{eq,p}$ (10), and calculated the equilibrium dose-pitch product $\widehat{D}_{eq}$, defined as $p \cdot D_{eq}$. The equilibrium dose-pitch product was calculated as mean for all pitches.

Table 4 - Metrics for scanner of General Electric

		Center				Peripheral					
Voltage (kV)	pitch	D_{eq} **(mGy)**	L_{eq} **(cm)**	α	$\widehat{D}_{eq}$ **(mGy)**	D_{eq} **(mGy)**	L_{eq} **(cm)**	α	$\widehat{D}_{eq}$ **(mGy)**	D_w **(mGy)**	$\widehat{D}_{eq.w}$ **(mGy)**
					Head						
80	0.531	9.6(0.4)	43.8(1.8)	0.96(4)	4.9(0.3)	9.1(0.4)	26.3(1.1)	0.77(3)	4.9(0.3)	9.3(0.3)	4.9(0.2)
	0.969	4.8(0.2)	40.3(1.6)	0.95(4)		5.0(0.2)	26.4(1.1)	0.78(3)		5.0(0.1)	
100	0.531	19.2(0.8)	46.3(1.9)	0.96(4)	10.0(0.6)	17.2(0.7)	33.0(1.3)	0.71(3)	9.2(0.5)	17.9(0.5)	9.5(0.4)
	0.969	10.1(0.4)	44.0(1.8)	0.96(4)		9.5(0.4)	32.7(1.3)	0.73(3)		9.7(0.3)	
120	0.531	32.6(1.3)	52.0(2.1)	0.96(4)	17.3(1.0)	30.3(1.2)	40.3(1.6)	0.66(3)	15.1(0.9)	31.0(0.9)	15.8(0.7)
	0.969	17.9(0.7)	52.1(2.1)	0.95(4)		14.5(0.6)	241(1.0)	1.11(4)		15.6(0.5)	
140	0.531	46.7(0.9)	50.8(2.0)	0.95(4)	24.4(1.4)	35.8(1.4)	29.7(1.2)	0.77(3)	19.7(1.1)	39.4(1.1)	21.2(0.9)
	0.969	24.8(1.0)	48.0(1.9)	0.96(4)		21.0(0.8)	37.0(1.5)	0.74(3)		22.3(0.6)	
					Body						
80	0.516	8.0(0.3)	43.5(1.7)	0.99(4)	4.2(0.2)	7.9(0.3)	28.6(1.1)	0.74(3)	4.9(0.2)	7.9(0.2)	4.3(0.2)
	0.984	4.4(0.2)	45.9(1.8)	0.99(4)		4.6(0.2)	39.2(1.6)	0.56(2)		4.5(0.1)	
100	0.516	18.8(0.8)	51.9(2.1)	0.98(4)	9.6(0.5)	16.8(0.7)	38.3(1.5)	0.73(3)	9.2(0.5)	17.4(0.5)	9.2(0.4)
	0.984	9.6(0.4)	50.1(2.1)	0.98(4)		9.4(0.4)	36.4(1.5)	0.80(3)		9.5(0.3)	
120	0.516	31.2(1.2)	53.2(2.0)	1.00(4)	16.1(0.9)	27.1(1.1)	43.4(1.6)	0.70(3)	15.1(0.8)	28.5(0.8)	15.0(0.6)
	0.984	16.3(0.7)	53.4(2.1)	0.97(4)		15.3(0.6)	47.9(1.9)	0.56(2)		15.6(0.5)	
140	0.516	45.6(1.8)	54.3(2.2)	0.97(4)	23.5(1.3)	39.4(1.6)	46.0(1.8)	0.74(3)	19.7(1.1)	41.5(1.2)	21.0(0.9)
	0.984	23.9(1,0)	54,3(2,2)	0.97(4)		19,4(0,8)	46,7(1,9)	0.73(3)		20.9(0,6)	

Font: The authors (2022).

Table 5 - Metrics for scanner of Toshiba

		Center				Peripheral					
Voltage (kV)	pitch	D_{eq} **(mGy)**	L_{eq} **(cm)**	α	$\widehat{D}_{eq}$ **(mGy)**	D_{eq} **(mGy)**	L_{eq} **(cm)**	α	$\widehat{D}_{eq}$ **(mGy)**	D_w **(mGy)**	$\widehat{D}_{eq.w}$ **(mGy)**
					Head						
	0.656	4.1(0.2)	18.2(0.7)	0.99(4)		9.2(0.4)	24.9(1.0)	0.72(3)		7.5(0.3)	
80	0.844	4.7(0.2)	27.8(1.1)	0.96(4)	3.9(0.3)	7.1(0.3)	23.5(0.9)	0.81(3)	6.1(0.4)	6.3(0.2)	5.4(0.2)
	1.406	3.6(0.1)	36.7(1.5)	0.94(4)		4.5(0.2)	23.9(1.0)	0.81(3)		4.2(0.1)	
	0.656	17.7(0.7)	45.1(1.8)	0.96(4)		17.4(0.7)	30.9(1.2)	0.70(3)		17.5(0.5)	
100	0.844	14.0(0.6)	46.2(1.8)	0.94(4)	11.5(0.8)	13.6(0.5)	30.4(1.2)	0.67(3)	11.4(0.8)	13.7(0.4)	11.4(0.3)
	1.406	8.0(0.3)	43.4(1.7)	0.95(4)		8.0(0.3)	31.4(1.3)	0.68(3)		8.0(0.2)	
	0.656	25.3(1.0)	40.0(1.6)	0.96(4)		26.4(1.1)	30.5(1.2)	0.67(3)		26.1(0.8)	
120	0.844	16.6(0.7)	33.1(1.3)	0.98(4)	16.3(1.1)	18.1(0.7)	20.0(0.8)	0.75(3)	16.9(1.2)	17.6(0.5)	16.7(0.5)
	1.406	13.0(0.5)	45.1(1.8)	0.95(4)		12.8(0.5)	34.2(1.4)	0.59(2)		12.9(0.4)	
	0.656	39.1(1.6)	48.8(2.0)	0.94(4)		36.4(1.5)	37.1(1.5)	0.67(3)		37.3(1.1)	
135	0.844	30.5(1.2)	48.7(1.9)	0.95(4)	25.8(1.8)	27.8(1.1)	35.8(1.4)	0.66(3)	23.6(1.6)	28.7(0.8)	24.3(0.7)
	1.406	18.5(0.7)	49.0(2.0)	0.95(4)		16.6(0.7)	36.5(1.5)	0.69(3)		17.2(0.5)	
					Body						
	0.641	11.1(0.4)	45.6(1.8)	0.96(4)		11.1(0.4)	20.3(0.8)	0.68(3)		11.1(0.3)	
80	0.828	8.4(0.3)	44.5(1.8)	0.96(4)	7.1(0.5)	9.8(0.4)	25.6(1.0)	0.87(3)	7.2(0.5)	9.4(0.3)	7.2(0.2)
	1.484	4.8(0.2)	45.9(1.8)	0.96(4)		-	-	-		4.5(0.1)	
	0.641	21.2(0.8)	49.1(2.0)	0.96(4)		22.8(0.9)	36.8(1.5)	0.65(3)		22.3(0.7)	
100	0.828	16.4(0.7)	48.8(2.0)	0.97(4)	13.5(0.9)	17.5(0.8)	32.7(1.3)	0.70(3)	15.0(1.0)	17.2(0.5)	14.5(0.4)
	1.484	9.2(0.4)	49.2(2.0)	0.95(4)		-	-	-		-	
	0.641	33.3(1.3)	51.0(2.0)	0.96(4)		34.4(1.4)	40.4(1.6)	0.64(3)		34.0(1.0)	
120	0.828	25.7(1.0)	50.9(2.0)	0.95(4)	21.2(1.5)	26.3(1.1)	29.0(1.2)	0.77(3)	22.3(1.6)	26.1(0.8)	21.9(0.7)
	1.484	14.4(0.6)	51.2(2.0)	0.95(4)		-	-	-		-	
	0.641	43.5(1.7)	52.1(2.1)	0.95(4)		41.5(1.7)	32.9(1.3)	0.96(4)		42.1(1.2)	
135	0.828	33.6(1.3)	51.9(2.1)	0.96(4)	27.7(1.9)	33.2(1.3)	38.3(1.5)	0.70(3)	26.7(1.9)	33.1(1.0)	27.0(0.8)
	1.484	18.7(0.7)	52.2(2.1)	0.95(4)		-	-	-		-	

Font: The authors (2022).

Table 6 - Metrics for scanner of Philips

		Center				Peripheral					
Voltage (kV)	**pitch**	D_{eq} **(mGy)**	L_{eq} **(cm)**	α	$\widehat{D}_{eq}$ **(mGy)**	D_{eq} **(mGy)**	L_{eq} **(cm)**	α	$\widehat{D}_{eq}$ **(mGy)**	D_w **(mGy)**	$\widehat{D}_{eq.w}$ **(mGy)**
					Head						
80	0.670	3.2(0.1)	47.7(1.9)	0.99(4)	2.5(0.1)	3.2(0.1)	24.6(1.0)	0.88(4)	2.5(0.1)	3.2(0.1)	2.5(0.1)

	0.893	3.2(0.1)	49.6(2.0)	0.98(4)		3.3(0.1)	37.4(1.5)	0.63(3)		3.3(0.1)	
100	0.670	6.9(0.3)	50.5(2.0)	0.99(4)	5.5(0.2)	6.6(0.3)	39.3(1.6)	0.70(3)	5.2(0.1)	6.7(0.2)	5.3(0.1)
	0.893	7.2(0.3)	52.8(2.1)	0.98(4)		6.6(0.3)	27.4(1.1)	0.82(3)		6.8(0.2)	
	0.670	12.3(0.5)	54.3(2.2)	0.97(4)		11.0(0.4)	37.8(1.5)	0.79(3)		11.5(0.3)	
120	0.893	12.2(0.5)	54.3(2.2)	0.98(4)	9.6(0.4)	11.7(0.5)	42.2(1.7)	0.75(3)	8.9(0.4)	11.9(0.4)	9.1(0.3)
	1.173	12.3(0.5)	54.3(2.2)	0.97(4)		11.7(0.5)	42.0(1.7)	0.78(3)		11.9(0.4)	
140	0.670	18.2(0.7)	55.1(2.2)	0.97(4)	14.2(0.4)	16.8(0.7)	40.4(1.6)	0.80(3)	13.2(0.4)	17.3(0.5)	13.5(0.3)
	0.893	18.2(0.7)	55.3(2.2)	0.96(4)		16.9(0.7)	49.1(2.0)	0.64(3)		17.3(0.5)	
Body											
	0.643	3.1(0.1)	47.8(1.9)	0.98(4)		3.1(0.1)	33.6(1.3)	0.72(3)		3.1(0.1)	
80	0.983	3.3(0.1)	49.6(2.0)	0.99(4)	3.0(0.1)	3.1(0.1)	33.6(1.3)	0.83(3)	3.3(0.1)	3.2(0.1)	3.2(0.1)
	1.173	3.3(0.1)	50.6(2.0)	0.97(4)		4.0(0.2)	46.7(1.9)	0.94(4)		3.8(0.2)	
	0.643	7.1(0.3)	52.0(2.1)	0.98(4)		6.9(0.3)	35.6(1.4)	0.81(3)		7.0(0.2)	
100	0.983	7.2(0.3)	53.0(2.1)	0.97(4)	6.7(0.2)	7.3(0.3)	45.0(1.8)	0.59(3)	6.3(0.2)	7.3(0.3)	6.4(0.2)
	1.173	7.2(0.3)	52.9(2.1)	0.98(4)		6.2(0.2)	29.4(1.2)	0.89(4)		6.5(0.3)	
	0.643	11.8(0.5)	51.8(2.1)	0.98(4)		11.3(0.5)	36.4(1.5)	0.76(3)		11.4(0.3)	
120	0.983	12.2(0.5)	54.3(2.2)	0.98(4)	11.3(0.4)	12.1(0.5)	48.4(1.9)	0.59(2)	11.5(0.4)	12.2(0.5)	11.4(0.3)
	1.173	12.3(0.5)	54.3(2.2)	0.97(4)		13.1(0.5)	50.7(2.0)	0.53(2)		12.8(0.6)	
	0.643	18.1(0.7)	55.1(2.2)	0.97(4)		16.1(0.6)	40.0(1.6)	0.77(3)		16.8(0.4)	
140	0.983	18.2(0.7)	55.1(2.2)	0.97(4)	17.0(0.6)	16.2(0.6)	45.3(1.8)	0.83(3)	16.2(1.6)	16.9(0.6)	16.4(0.4)
	1.173	18.3(0.7)	55.2(2.2)	0.96(4)		18.9(0.8)	46.0(1.8)	0.74(3)		18.7(0.9)	

Font: The authors (2022).

4. Discussion

From the measurements, the metrics D_{eq}, α and L_{eq} were obtained using the single method, as described on AAPM Task Group 200. Different clinical protocols (pitch, voltage, head/body, center/peripheral) were used for scanners of different vendors. Varying those protocols, the metrics D_{eq}, α and L_{eq} are changes. The increase of pitch results on the decrease of D_{eq}. It makes sense because the increase of pitch results on the increase of velocity. As well as the increase of voltage results on the increase D_{eq}.

Considering the quantities α and L_{eq}, they tend to be higher for central then peripheral measures. Considering that the X-ray undergoes more scatter-to-primary ratio on center then peripheral (4), so it makes sense that the scatter fraction, α, is higher for center.

5. Conclusion

On the present work, the metrics D_{eq}, L_{eq} and α were obtained from a single scanning length (single method), using a real-time dosimeter. From the single scanner, the whole curve dose in function of the scanning length was acquired, without the need of several scanners.

Applying the method described on AAPM report 200, which consists on algebraic manipulation the Eq. 1, the metrics were obtained, including the dose for an ideal infinite large phantom. So the use of the ICRU/AAPM phantom can obtain the dose without underestimating it, being a good alternative beyond $CTDI_{100}$, whose measurements is a scanning length of 100 mm.

Comparing the values for $\widehat{D}_{eq.w}$, the dose delivered by Toshiba scanner is higher than GE and Philips, for head and body filters. On the other hand, the dose for Philips scanner is the smallest for head and body filters. GE is the only, of the three scanners, whoso dose for head filter is higher than body filter.

Acknowledgment

The authors thanks to the technical, from the mechanical workshop from Institute of Physics, USP, for manufacturing the phantom.

References

1. Dixon RL. The Physics of CT Dosimetry: CTDI and Beyond. 1st ed. Boca Raton: CRC Press; 2019.
2. AAPM. The Measurement, Reporting, and Management of Radiation Dose in CT. American Association of Physicists in Medicine. 2008;AAPM Report 096.
3. Boone JM. The trouble with CTDI100. Medical Physics. 2007;34(4):1364-71.
4. AAPM. Comprehensive Methodology for the Evaluation of Radiation Dose in X-Ray Computed Tomography. American Association of Physicists in Medicine. 2010;AAPM Report 111.
5. ICRU. Radiation Dosimetry and Image Quality Assessment in Computed Tomography. International Commission on Radiation Units and Measurements. 2012;Report 87.
6. AAPM. The Design and Use of the ICRU/AAPM CT Radiation Dosimetry Phantom: An Implementation of AAPM Report 111. American Association of Physicists in Medicine. 2020;AAPM Report 200.
7. Costa PR, Nersissian DY, Umisedo NK, Gonzales AHL, Fernandez-Varea JM. A comprehensive Monte Carlo study of CT dose metrics proposed by the AAPM Reports 111 and 200. Medical Physics. 2022;49(1):201-18.
8. Dixon RL, Ballard AC. Experimental validation of a versatile system of CT dosimetry using a conventional ion chamber: beyond CTDI100. Medical physics. 2007;34(8).
9. Radcal Corporation. 10X6-0.6C: The Chamber for Computed Tomography Dose Index (CTDI); 2011.
10. Leitz W, Axelsson B, Szendro G. COMPUTED-TOMOGRAPHY DOSE ASSESSMENT - A PRACTICAL APPROACH. Radiation Protection Dosimetry. 1995;57(1-4):377-80.

Contact:

Paulo Roberto Costa
Group of Dosimetry of Radiation and Medical Physics
Department of Nuclear Physics - Institute of Physics of USP
pcosta@if.usp.br